PERGAMON

International Journal of Multiphase Flow 27 (2001) 1415–1430

International Journal of Multiphase Flow

www.elsevier.com/locate/ijmulflow

Visual observations of flooding in narrow rectangular channels

N.A. Vlachos, S.V. Paras, A.A. Mouza, A.J. Karabelas *

Department of Chemical Engineering, and Chemical Process Engineering Research Institute, Aristotle University of Thessaloniki, Univ. Box 455, Thessaloniki, GR-540 06, Greece

Received 16 December 1999; received in revised form 8 August 2000

Abstract

New flooding data in a vertical rectangular channel with 5 and 10 mm gap between its main parallel plates are reported. Visual observations and fast recordings are made to determine conditions associated with the onset of flooding in the channel. For the 10 mm gap channel a combination of mechanisms, i.e., levitation and upward transportation of laterally coherent or isolated waves, and local wave bridging, appear to be responsible for triggering flooding. The critical flooding velocity is curiously nearly independent of liquid flow rate above film Reynolds number approximately 500. In the 5 mm gap channel and for small Re_L, flooding occurs at the liquid entrance, whereas "massive" wave bridging, occurring above the middle of the test section, is the dominant flooding mechanism for relatively higher Re_L. Predictions based on small amplitude stability analysis are in good agreement with flooding data from the latter case.

Keywords: Flooding; Countercurrent flow; Air–water flow; Vertical rectangular channel; Narrow gap; Visual studies

1. Introduction

In countercurrent gas–liquid flow, flooding is defined as the condition at which liquid is carried above the point of its entry; i.e., a situation where at least part of the liquid flow is reversed in direction. The countercurrent flow limitation (CCFL) or onset of flooding is identified as the maximum rate at which one phase can flow counter-currently with respect to the other. The phenomenon of flooding is of considerable technological importance being a limiting factor for the operation of various types of two-phase equipment including the very common reflux condensers. In the latter, flooding poses a major problem, hindering their smooth operation. It is associated with choking of the upward moving vapors and with a sharp rise of pressure drop. In

* Corresponding author. Tel.: +30-31-996201; fax: +30-31-996209.
E-mail address: karabaj@cperi.certh.gr (A.J. Karabelas).

0301-9322/01/$ - see front matter
PII: S0301-9322(01)00009-X

the case of modern *compact condensers* this problem is aggravated by the narrow flow passages between plates. Therefore, the design engineer needs reliable tools to determine the critical conditions leading to flooding as well as the region of smooth condenser operability. Such tools are unavailable at present mainly due to very limited work reported for narrow flow passages, in particular of rectangular cross-section. Therefore, it is the purpose of this work to study flooding, under adiabatic conditions, in a uniform vertical rectangular channel with relatively small gaps, between the main parallel plates, i.e., 5 and 10 mm. Such a channel is considered to simulate, albeit in a simplified manner, a single flow "element" of a compact condenser.

In a rather comprehensive paper, Bankoff and Lee (1986) reviewed the experimental evidence as well as the mathematical models and empirical correlations proposed for flooding phenomena in vertical countercurrent flow. This review as well as recent investigations (e.g., Govan et al., 1991; Lacy and Dukler, 1994; Zapke and Kroeger, 1996; Koizumi and Ueda, 1996; Ghiaasiaan et al., 1997; Wongwises and Thanaporn, 1998; etc.) show that the main factors influencing the onset of flooding are (in addition to the physical properties of both fluids):

- the geometry of the conduit (tube or rectangular channel), its dimensions and angle of inclination;
- the type of liquid and gas entrance and exit.

In fact, the mechanism by which flooding occurs is apparently dependent on all these factors and although the importance of the phenomenon has led to extensive studies, there is still a great deal of uncertainty concerning the exact mechanism responsible for triggering it. Researchers of flooding mechanisms (e.g., Zabaras, 1985; No and Jeong, 1996) tend to classify them into three broad categories; i.e., wave dynamics (flooding due to instability of interfacial waves), film dynamics (based on the concept of upward motion in the film) and drop dynamics (entrainment of liquid influencing the flooding process). Recently, Hewitt (1995) also identified the wave mechanism (levitation of a large interfacial wave and its subsequent upward motion due to gas action) and the entrainment mechanism, as the two prevailing mechanisms responsible for the onset of flooding. All the aforementioned flooding studies were made in circular tubes, with relatively large diameters (above 10 mm), and unclear results regarding the dominant mechanism (e.g., Hewitt, 1995). Interesting flooding models have been developed based on assumed interfacial shapes, i.e., the stationary wave model by Shearer and Davidson (1965) and the roll wave model proposed by Richter (1981).

Very few flooding studies with rectangular channels are available. Biage (1989) conducted flooding tests in a 250 mm wide vertical channel with porous liquid inlet and outlet sections. The channel gap between the main parallel plates was relatively large (25 mm). According to Biage, flooding occurred through droplet entrainment from standing waves, near the liquid inlet, and it was not associated with large wave upward transportation beyond the point of liquid entry. Biage observed that some large waves did start moving upwards, but (almost immediately) fell downward and vanished. It will be pointed out, however, that the 25 mm gap in that study is considered large compared to the setup used here. Osakabe and Kawasaki (1989) carried out "top flooding" experiments in thin rectangular passages (i.e., 10×100, 5×100 and 2×100 mm^2) motivated by problems in the nuclear industry (emergency reactor core cooling). Their flow system, however, with a pool of fluid (of constant head) above the channel top, is drastically different than the flow field studied here, where uniform liquid films are introduced at the channel walls. Tests with similar (constant static head) liquid feeding conditions, in very narrow rectangular channels of 1.1

and 2.2 mm gap, are reported by Larson et al. (1994). Ghiaasiaan et al. (1996) studied the effect of gas injection configuration on flooding in short vertical circular tubes with small internal diameters; namely 4.75, 11.9 and 19.1 mm. Regrettably, no specific reference was made concerning flooding mechanisms; thus one cannot directly compare their results with those of the present visual studies.

It will be noted that the most widely used form of correlation for estimating the onset of flooding in vertical tubes (although quite often unsuccessfully, Bankoff and Lee, 1986) is due to Wallis (1969):

$$\sqrt{U_G^*} + C_1 \sqrt{U_L^*} = C_2, \tag{1}$$

where

$$U_G^* = U_G \sqrt{\frac{\rho_G}{gD(\rho_L - \rho_G)}}, \tag{2}$$

$$U_L^* = U_L \sqrt{\frac{\rho_L}{gD(\rho_L - \rho_G)}} \tag{3}$$

with parameters $C_1 = 0.8$ to 1.0 and $C_2 = 0.7$ to 1.0, mainly depending on geometry. U_G and U_L are the gas and liquid superficial velocities, respectively, ρ_G and ρ_L the phase densities, g the acceleration due to gravity and D the tube diameter. This correlation, and variations thereof (e.g., Pushkina and Sorokin, 1969) imply that there is a linear relationship between $U_G^{1/2}$ and $U_L^{1/2}$, without theoretical backing.

As part of a project to study countercurrent flow through narrow passages and in view of the unsatisfactory state of the art, flow visualization studies were made in a vertical channel in order to gain insight into the complicated flow field and to elucidate the flooding mechanisms. In the following, the experimental configuration and procedures are outlined first; the main results drawn from the flooding tests and visualization studies are presented and discussed next.

2. Experimental setup

An experimental facility was specifically built to study countercurrent gas–liquid flow (or reflux flow) and to determine flooding conditions (Fig. 1). Two-phase flow is developed in a 70 cm high and 15 cm wide rectangular channel made of Plexiglas. The spacing between the two parallel plates may be varied in order to investigate its effect on the onset of flooding. Data are reported here for two different gaps, namely 5 and 10 mm. Air enters the device at the bottom through a specially made entrance section (i.e., honeycomb) to achieve well-developed conditions before it contacts the falling liquid film. Filtered tap water is introduced from the top and removed from the bottom via *porous sections* (covering the entire active channel width) embedded flash with the main flat surfaces. Thus, two porous wall sections (opposite one another) are used for feeding the water into the test channel and two for its removal. The inlet and the outlet sections are identical except that the water flow direction is reversed. The length of the test section, measured between the bottom edge of the inlet porous wall and the top edge of the outlet porous section, is 40 cm. A cross-sectional view of the test section is shown in Fig. 2. The equipment arrangement allows a

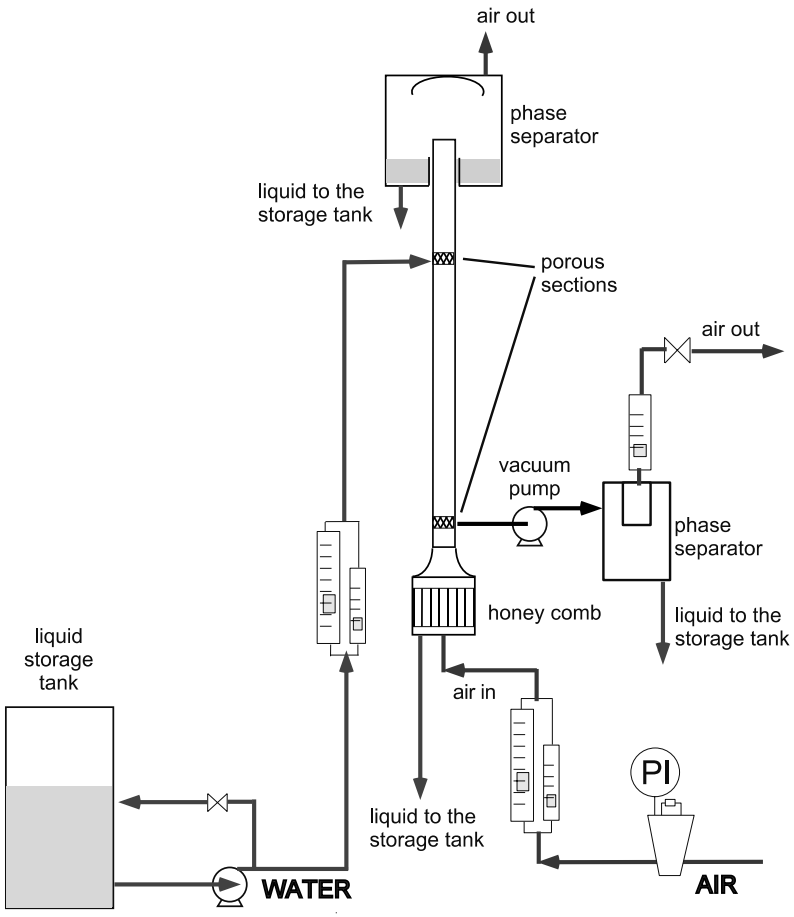

Fig. 1. A schematic of the experimental setup for studying countercurrent gas–liquid (reflux) flow.

sufficiently long calming section for the gas and minimizes the possibility of artificially creating disturbance waves due to the liquid exit geometry.

The liquid and gas flow rates are measured using a set of calibrated rotameters. A small amount of gas flows out together with the liquid film removed in the lower porous wall section. This gas flow rate is measured by a rotameter after separating the two fluids using a phase separator and a vacuum pump. The latter is also used to produce, together with a slightly elevated pressure inside the measuring section, the necessary driving force in order to suck the liquid through the exit porous wall section. The amount of gas removed with the liquid varies between 3% and 10% of the gas inlet flow rate. The removed-gas flow rate is subtracted from that of the inlet gas in order to determine the true gas flow rate employed in the flooding experiments. Pressure drop is measured over the test section using an electronic differential pressure transmitter connected to two pressure taps. The water is collected in a 50 l storage tank and is recirculated through the loop by means of a centrifugal pump. On top of the measuring section there is a phase separator from which the liquid phase is fed back to the storage tank, whereas air is released to the atmosphere. This setup

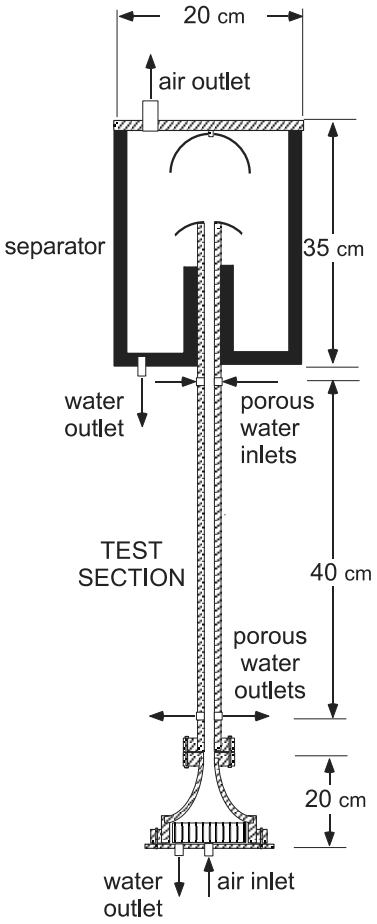

Fig. 2. Cross-sectional view of the test section.

allows good control of flow conditions and represents an idealized case of conditions prevailing in a single element of a compact heat exchanger.

3. Experimental conditions and procedure

The experiments were carried out at a slightly elevated pressure (up to 1.1 bar absolute) maintained inside the test section, to facilitate liquid removal through the outlet porous wall section. The selected range of flow rates was $Q_L = 0$ to 7 l/min for the water and $Q_G = 3$ to 20 l/s for the air. During the main series of flooding tests, air and water were at ambient temperature (approx. 20°C). It should be added that the inner surface of the Plexiglas test section was very smooth and its wettability was improved by treating it (before each set of experiments) with a silica sol.

Each experiment is carried out by pre-pressurizing the channel with the gas flowing at a relatively low rate. Then, the required liquid flow rate is fixed and steady liquid film flow is estab-

lished, down to the outlet porous wall section where it exits the channel. Following this, the gas flow rate is progressively increased until the onset of flooding. It is noteworthy that the occurrence of flooding coincides with a rather sharp increase of the pressure drop level. Care has to be exercised to avoid triggering flooding by rapid operation of the valve controlling the air inlet flow rate.

The onset of flooding is defined as the condition at which the liquid on the channel wall begins to move partially above the liquid injection section. Thus, direct visual observations are a significant part of the experiments aimed at gaining insight into the basic mechanisms triggering flooding. Visual studies were made using a Redlake *Motion* Scope PCI® high-speed camera positioned outside the test section, either slightly above the liquid exit or below the liquid entrance section. Recordings were made from two angles; i.e., first by aligning the camera normal to one of the channel main parallel plates and then (turning 90°) by viewing between the plates, inside the gap. Moreover, placing a reflecting plate at a certain vertical position near the channel, made it possible to better analyze the onset of flooding by recording high-speed digital images of the flow, captured from the channel front and side simultaneously. The imaging system used is capable of recording up to 1000 full frames per second, whereas for the present experiments 500 fps is considered to be a suitable recording rate.

4. Results

Fig. 3 provides an overview of the observed flooding conditions for the 5 and 10 mm gaps. The rather strong influence of gap dimensions on critical flooding velocity is evident. The data show

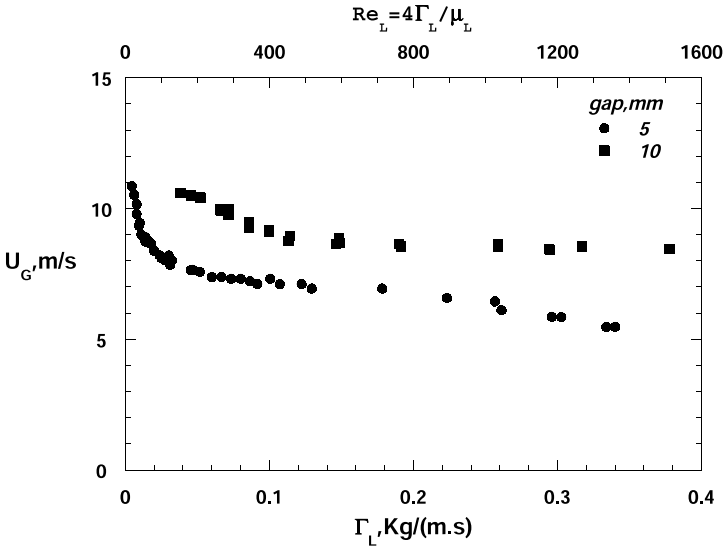

Fig. 3. Superficial gas velocity plotted vs the liquid mass flow rate per unit length of channel circumference, Γ_L, and the corresponding liquid Re_L, at the onset of flooding.

that for relatively low liquid flow rates Γ_L (i.e., liquid mass flow rate per unit length of channel circumference), the critical superficial gas velocity, U_G, tends to increase with decreasing liquid flow rate. However, over a broad range of relatively high liquid flow rates, this critical gas velocity remains nearly constant in the case of 10 mm gap and it is a weak function of Γ_L for the 5 mm channel. A nearly constant gas flooding velocity at relatively high liquid flow rates is also presented by O'Brien et al. (1986). They report air/water flooding data obtained in a 50.8 mm i.d. vertical tube, which is relatively large compared to the setup employed here. A subsequent careful account of visual observations is required to offer an interpretation of the new data.

As is well-known, at small Re_L numbers the liquid film is very thin and laminar. Here Re_L is defined as $4\Gamma_L/\mu_L$, where μ_L is the liquid viscosity. The picture in Fig. 4(a) is an example of liquid film development (near the liquid entrance) at small gas flow rates, far below critical conditions. The film surface appears to be initially smooth and undisturbed. Downstream nearly two-dimensional disturbances develop first, evolving into a three-dimensional, small-amplitude wave structure. These waves are characterized by (somewhat faster moving) pebble-like wave fronts, clearly identified in the picture. This behavior is similar to that observed in free falling films.

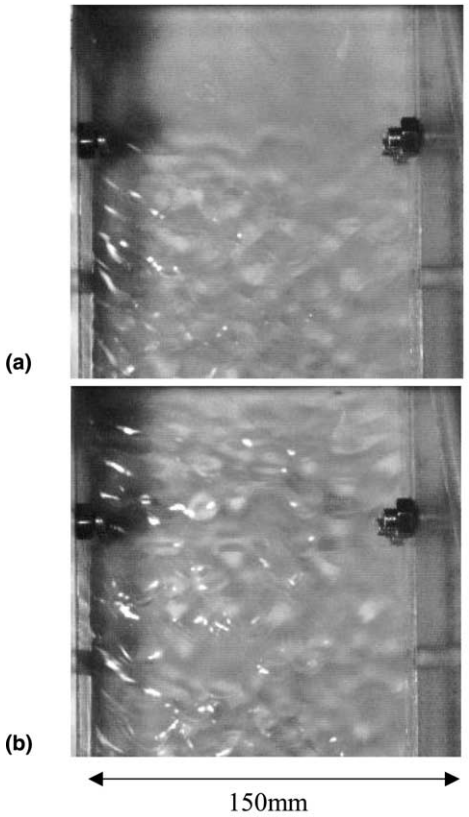

Fig. 4. Liquid film flow on the channel main parallel plate: (a) for very low gas velocities and (b) for increased gas velocities, still well below critical flooding conditions.

Fig. 4(a) is typical of both 5 and 10 mm channel flow at small liquid and gas feed rates. This picture provides also evidence that there is a uniform liquid film spreading (at the liquid entry section) in the present experimental setup. However, it is suspected that at the bottom edge of the porous entry section the film is slightly thicker, than immediately downstream, due to liquid loading. This slight thickness increase may have an influence on flooding at small liquid rates, as discussed below.

At fixed small liquid rate, by increasing the gas flow rate (Fig. 4(b)) the wave disturbance on the film surface moves upstream, covering the entire film surface up to the liquid entry. With increasing distance downstream, gravity aids wave growth (as is well-known) especially at high liquid rates.

4.1. Observations in 10 mm-gap channel

At this comparatively larger gap, increased superficial gas velocities are required to effect a sufficiently strong gas/liquid interaction leading to flooding (Fig. 3). A notable feature of this dynamic interaction (at a critical gas rate), are the fairly coherent large waves, covering a large portion of the channel width (Fig. 5), which seem to be momentarily arrested near the *liquid exit* by the counter-currently flowing gas. The terms "standing wave" or "wave levitation" (Hewitt, 1995) may be appropriate in this case. Such large disturbance waves appear intermittently and are swept up the channel, passing beyond the liquid injector and generating a sustained concurrent up-flow. This condition is considered as the onset of flooding. In the region above the liquid entry section, a concurrent churn type flow is created.

Similar observations of wave levitation were made by McQuillan et al. (1985), even though they conducted flooding tests in an entirely different geometry; i.e., flooding occurred in the annulus formed by a vertical rod positioned centrally within a perspex tube. Porous liquid inlets and outlets were also employed in that study. However, for the 10 mm gap channel of the present

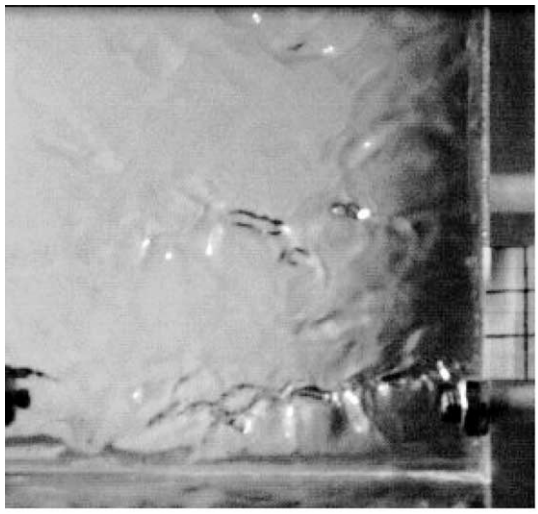

Fig. 5. "Coherent" wave, covering almost the entire channel width. Side view of the channel; 10 mm gap, $Re_L = 400$.

study, the "wave levitation" mechanism is not very pronounced. More specifically, due to the relatively large channel width (15 cm), upward movement of a laterally coherent wave, as an entity, from the region at the lower porous section to that at the liquid inlet and beyond, does not seem feasible. This observation is in agreement with Jayanti et al. (1996) who remark that in tubes with large diameter, a circumferentially coherent wave cannot be easily formed. Indeed, even if such a wave is momentarily formed, it apparently cannot be transported (as a whole) over a significant distance, displaying a tendency to become unstable and to break up.

Upon close examination of recordings, the following elementary mechanisms are identified at the onset of flooding. *"Isolated" waves* covering part of the liquid film surface in the lateral direction, are swept up the channel, due to the drag and pressure forces exerted by the gas flow. Some of these isolated waves are seen to be formed when the coherent large wave (mentioned above) breaks up into smaller ones as it moves upwards. Furthermore, *entrained liquid droplets*, torn off the surface waves, are observed to follow the gas upflow. Additionally, when focusing in-between the main plates (into the gap), one can observe that some waves on the liquid film surface tend to become unstable with their amplitude rapidly increasing (possibly due to interfacial shear) till they partially block the gap (i.e., *local bridging*), thus reducing the cross-sectional area available to gas flow. The liquid of these waves is then forced by the gas to accelerate upwards (beyond the liquid inlet), having a slug form with some entrained droplets. This sequence of events is clearly depicted in Fig. 6. After flooding is established, concurrent flow above the liquid inlet zone coexists with some countercurrent flow below. The liquid rate in the latter is insufficient to sustain flooding.

Several additional remarks are worth making concerning flow in the 10 mm gap channel:

- incipient flooding is observed in the *lower* half of the channel, mostly close to the liquid exit area;

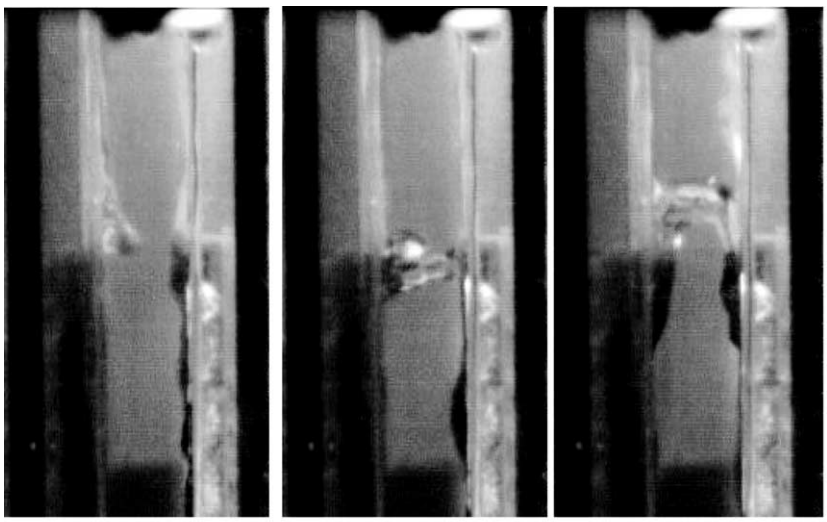

Fig. 6. The "wave bridging" mechanism. View between the main parallel plates, inside the 10 mm gap ($Re_L = 400$).

- the mechanism involving isolated waves appears to dominate at low Re_L, whereas "1ocal bridging" is dominant over most of the (high) Re_L range;
- entrained droplets are of low concentration and do not seem to play a significant role in flooding narrow channels, unlike other cases with relatively large diameters or gaps (e.g., Biage, 1989);
- the trend of flooding data shown in Fig. 3 is not unexpected for low liquid rates. However, the nearly constant critical U_G at high liquid rates is somewhat surprising and difficult to explain. One may speculate that beyond a certain liquid rate (e.g., $\Gamma_L > \sim 0.15$) the disturbance waves attain a limiting height requiring a nearly constant gas flow rate to cause local bridging.

4.2. Flooding in a 5 mm-gap channel

The small gap size is the determining factor in this case, in that the proximity of the two wavy liquid films facilitates bridging and flooding. Indeed, the observations reveal that, at Re_L greater than ~ 150, "wave bridging" is the dominant mechanism responsible for flooding phenomena. By increasing the gas velocity, waves on the liquid film surface grow as they move downwards, form liquid bridges and block this smaller gap before they reach the middle of the test section. For flow conditions very close to the onset of flooding, it is estimated that the mean liquid wave height, h_w, becomes comparable to the 5 mm gap, as shown in Fig. 7; indeed mean wave height at each parallel channel plate approaches values of about 2 mm, for relatively high liquid flow rates. In Fig. 7, the wave height is considered to be roughly equal to four times the base film thickness, h (e.g., Karapantsios et al., 1989; No and Jeong, 1996); h is obtained from the well-known Nusselt (1916) formula. According to Zabaras (1985), the liquid film attains, as expected, even higher thickness values than those estimated by the Nusselt expression, when approaching the critical

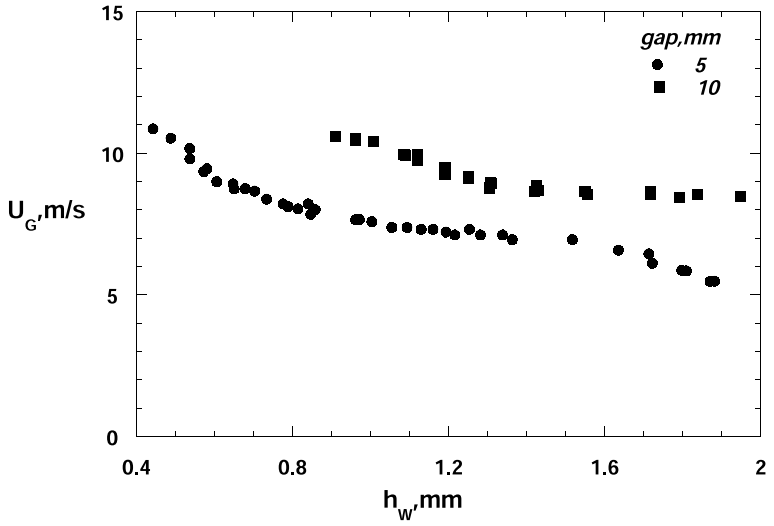

Fig. 7. Superficialgas velocity plotted versus an estimate of liquid wave height, at flow conditions very close to the onset of flooding.

flooding conditions. Therefore, blocking of the channel gap occurs at lower gas flow rates and smaller growth of disturbance waves (due to gas/liquid interaction) compared to the 10 mm plate spacing. For the 5 mm gap case, a particular flow pattern develops at the flooding point, comprised of large unstable liquid masses with gas bubbles trapped therein, blocking the channel gap (''massive'' bridging) and bouncing up and down probably due to air forcing its way upwards. The sequence of pictures in Fig. 8 is typical of such massive bridging at relatively high Re_L.

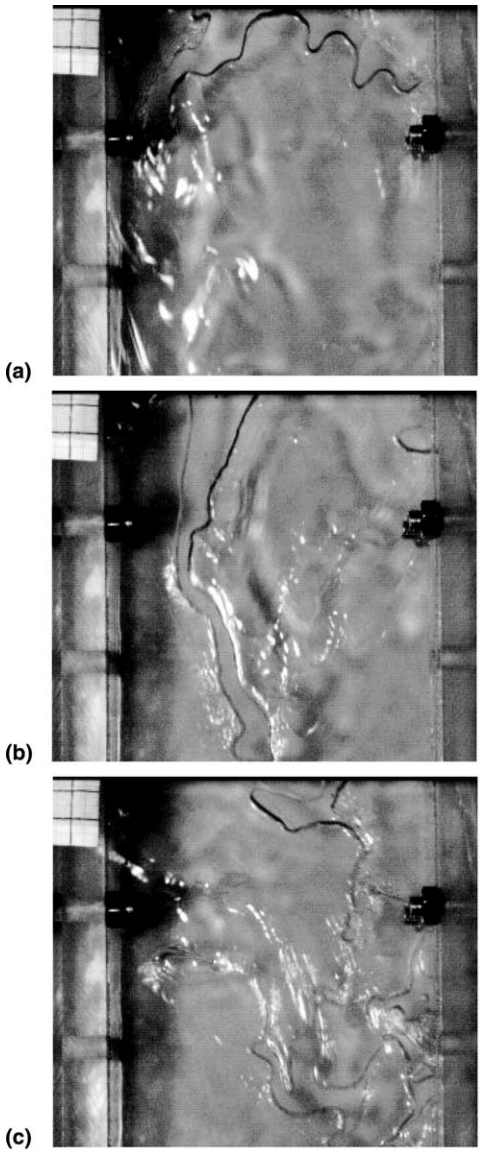

Fig. 8. Flooding phenomena in the 5 mm gap channel at $Re_L = 1360$ (side view): (a) liquid wave on the main channel plate starting to reverse its flow direction (time:0 ms), (b) gas penetrating liquid blocked channel gap (time: 400 ms), and (c) liquid masses blocking the channel gap with gas bubbles trapped (time: 1500 ms).

For low liquid flow rates (i.e., $Re_L < 150$), flooding is observed to occur at the liquid inlet. Fig. 9 includes a sequence of pictures showing incipient flooding near the *liquid inlet* section. This may be attributed to the fact that a rather small disturbance wave, formed near the liquid entry (despite precautions taken), grows and reverses its flow direction earlier than the small amplitude isolated waves, developing on the surface of the relatively thin film downstream. Most of these waves, even though they start moving downwards, are seen to slow down immediately and to reverse their flow

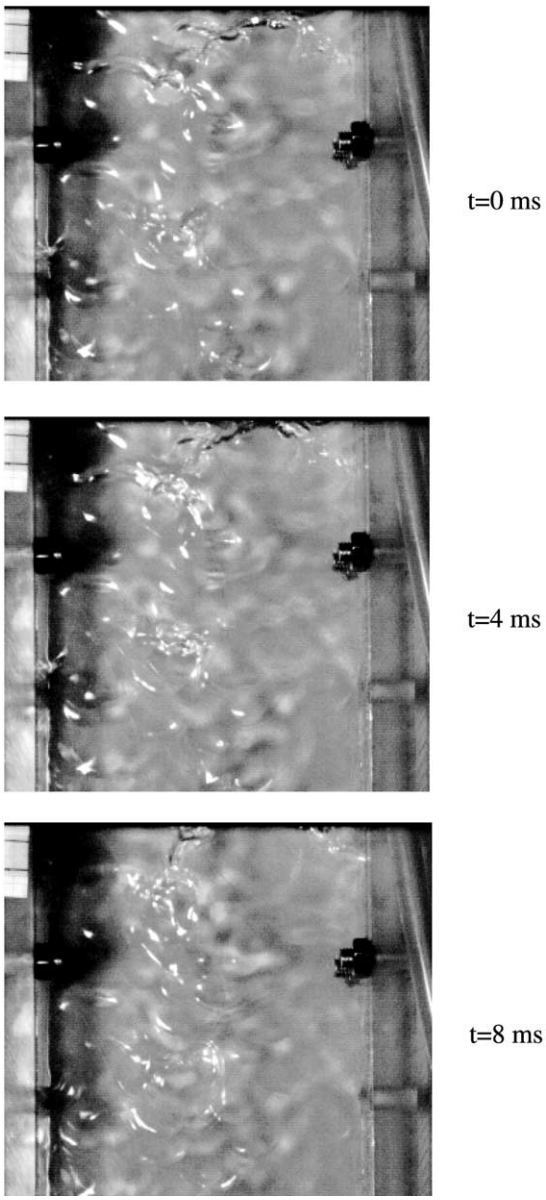

Fig. 9. Flooding near the liquid inlet porous section. Side view of the channel; 5 mm gap, $Re_L = 130$.

direction. Flooding near the liquid entrance was also observed by Biage (1989) and it was attributed to droplets ripped off the crests of large amplitude waves, which were created close to the liquid inlet as a result of an increasing gas velocity. It should be added that in the 10 mm gap channel, at relatively low liquid flow rates (and relatively high gas velocities), entrance flooding is not observed, since the larger spacing between the parallel plates allows the surface waves to grow as they move towards the liquid outlet. Thus, flooding (clearly related to such wave growth) occurs near the liquid exit. Still, in a few runs with 10 mm gap at low liquid velocity, entrance flooding was also observed together with exit flooding. According to No and Jeong (1996) entrance and exit flooding compete with each other and both may occur under certain conditions.

5. Discussion

It is difficult at present to propose a correlation covering both 5 and 10 mm gaps. Fig. 10, shows that a Wallis-type correlation would be unsuccessful; only at low liquid rate there is a semblance of linearity between $(U_G^*)^{1/2}$ and $(U_L^*)^{1/2}$. The fact that the data, plotted as in Fig. 10, come closer together might offer in the future (with the addition of more measurements) the possibility of proposing some rough guidelines on the critical U_G, for practical applications. It should be pointed out that to prepare Fig. 10, the channel gap is employed in Eqs. (2) and (3) (instead of tube diameter, D) as the characteristic length for computing U_G^* and U_L^*.

In the case of the small 5 mm gap, it was observed that a rather small growth of disturbance waves could lead to incipient flooding. Lacking a better model, it is not unreasonable to consider that instability of small-amplitude disturbances is the cause of flooding under these conditions. It is, therefore, tempting to compare the 5 mm data against the results of linear small amplitude stability analysis, such as that performed by Cetinbudaklar and Jameson (1969). This comparison is shown in Fig. 11, revealing that a fairly good agreement exists between the present flooding data

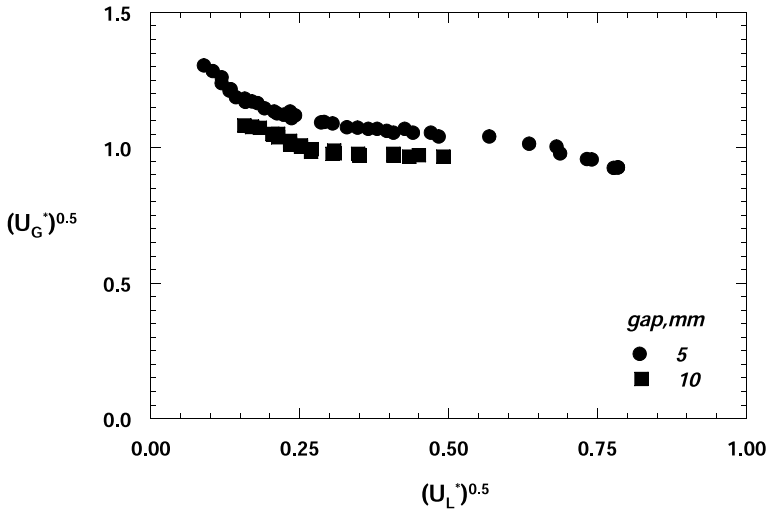

Fig. 10. Experimental flooding data for both the 5 and 10 mm gap channel cases.

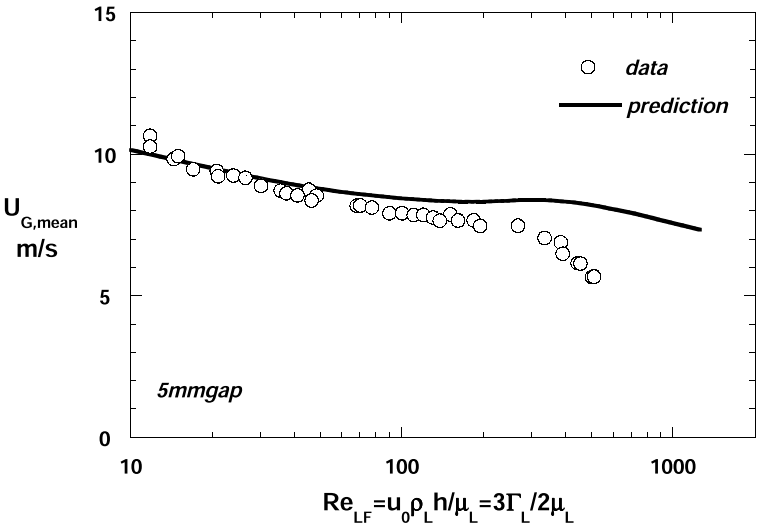

Fig. 11. Experimental flooding data compared to predictions, based on linear small amplitude stability analysis, made by Cetinbudaklar and Jameson (1969).

and the predictions of this linear stability analysis. According to Cetinbudaklar and Jameson, the failure of the theory for relatively large *Re* is due to the fact that the liquid film becomes turbulent, thus rendering the Nusselt parabolic velocity profile invalid. In Fig. 11, the mean gas velocity, $U_{G,mean}$, is calculated from the gas volume flow rate by first dividing it by the gas core area and then by subtracting the air/water interfacial velocity, u_0. The latter, estimated to be less than 5% of $U_{G,mean}$, is calculated (for laminar flow down a vertical wall under gravity) from the liquid film thickness, h, obtained using the Nusselt formula. The gas core area is estimated as the channel area minus the area occupied by the liquid film. The liquid film Re_{LF} is based on the film surface velocity u_0 and the liquid film thickness; i.e., $Re_{LF} = u_0 \rho_L h/\mu_L = 3\Gamma_L/2\mu_L$, where ρ_L is the liquid density.

In the case of the 10 mm gap, it was observed that standing waves are formed momentarily prior to flooding. It is, therefore, of interest to compare the flooding data with predictions from the Shearer and Davidson (1965) theoretical treatment of the standing wave. Fig. 12 shows that, overall, there is poor agreement between data and predictions. Only in the range of small $Re_L (< 500)$ the trend is the same, but the difference in critical velocity $U_{G,mean}$ measured and predicted varies between 10% and 20%. The very significant deviation observed at Re_L above ~500 may be attributed to the fact that the flooding mechanism of "local bridging", which is dominant in this high Re_L range, is different than the one considered in the Shearer and Davidson theoretical analysis. It should be noted that in this figure, the film surface velocity u_0 was not taken into account for the estimation of $U_{G,mean}$.

6. Concluding remarks

The reported visual observations and fast recordings show that the gap size plays a dominant role in flooding vertical rectangular channels. For the 5 mm gap channel and relatively high

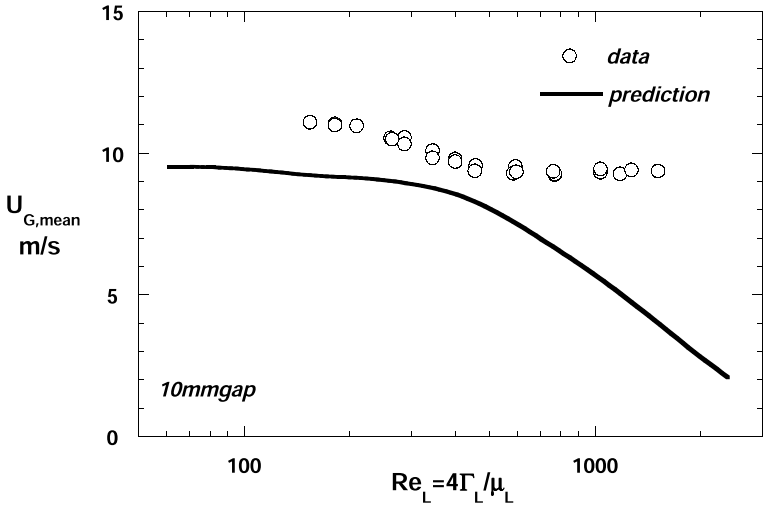

Fig. 12. Experimental flooding data compared to predictions, based on the "standing wave" model of Shearer and Davidson (1965).

$Re_L (> 150)$, "massive" wave bridging is the prevailing flooding mechanism brought about by moderate wave growth on the two films, flowing in close proximity, on opposite walls. It is interesting that there is very good agreement of the 5 mm data with predictions from linear small amplitude stability analysis (Cetinbudaklar and Jameson, 1969). For relatively small Re_L (i.e., below 150), with thin liquid films formed inside the test section, flooding is observed to occur at the liquid entry very likely due to growth of disturbances right below the porous section.

In the larger (10 mm) gap the picture is quite different. For relatively high liquid flow rates ($Re_L > 500$), the critical flooding gas velocity tends to be independent of liquid flow rate, which is difficult to explain. Although some wave "levitation" may take place (in the lower half of the test section), movement upward of "isolated" waves and "localized bridging" seem to be the main flooding mechanisms. The latter is quite pronounced. Droplet entrainment, although present, does not appear to contribute significantly to flooding. At smaller liquid flow rates ($100 < Re_L <\sim 500$) the mechanism involving isolated wave movement upward appears to dominate. In view of these observations one would expect that, in this low Re_L range, the "standing wave" model of Shearer and Davidson (1965) would perform well. The comparison of data with predictions shows the same qualitative trend, but a significant quantitative disagreement.

It is noted that the frequently used Wallis (1969) correlation is inapplicable to the data presented here. Furthermore, no single (all encompassing) model or correlation appears to be capable of coping with the different mechanisms and geometries. Additional work on countercurrent two-phase flow in narrow passages, for measuring detailed flow properties, is certainly required.

Acknowledgements

Financial support by the European Commission under contract JOE3-CT97-0062 is gratefully acknowledged.

References

Bankoff, S.G., Lee, S.C., 1986. A critical review of the flooding literature. In: Hewitt, G.F., Delhaye, J.M., Zuber, N. (Eds.), Multiphase Science and Technology. Hemisphere, New York, pp. 95–180 (Chapter 2).

Biage, M. 1989. Structure de la surface libre d'un film liquide ruisselant sur une plaque plane vertical et soumis a un contre-courant de gas: Transition vers l'ecoulement cocourant ascendant. Ph.D. Thesis, Inst. Nat. Polytechnique de Grenoble, France.

Cetinbudaklar, A.G., Jameson, G.J., 1969. The mechanism of flooding in vertical countercurrent two-phase flow. Chem. Eng. Sci. 24, 1669–1680.

Ghiaasiaan, S.M., Wu, X., Sadowski, D.L., Abdel-khalik, S.I., 1997. Hydrodynamic characteristics of counter-current two-phase flow in vertical and inclined channels: effects of liquid properties. Int. J. Multiphase Flow 23, 1063–1083.

Ghiaasiaan, S.M., Bohner, J.D., Abdel-Khalik, S.I., 1996. The effect of gas injection configuration on two-phase countercurrent flow limitation in short vertical channels. Nucl. Sci. Eng. 123, 136–146.

Govan, A.H., Hewitt, G.F., Richter, H.J., Scott, A., 1991. Flooding and churn flow in vertical pipes. Int. J. Multiphase Flow 17, 27–44.

Hewitt, G.F. 1995. In search of two-phase flow. In: Presented at 30th US National Heat Transfer Conference, Portland, Oregon.

Jayanti, S., Tokarz, A., Hewitt, G.F., 1996. Theoretical investigation of the diameter effect on flooding in countercurrent flow. Int. J. Multiphase Flow 22, 307–324.

Karapantsios, T.D., Paras, S.V., Karabelas, A.J., 1989. Statistical characteristics of free falling films at high Reynolds numbers. Int. J. Multiphase Flow 15, 1–21.

Koizumi, Y., Ueda, T., 1996. Initiation conditions of liquid ascent of the countercurrent two-phase flow in vertical pipes (in the presence of two-phase mixture in the lower portion). Int. J. Multiphase Flow 22, 31–43.

Lacy, C.E., Dukler, A.E., 1994. Flooding in vertical tubes – Part I: Experimental studies of the entry region. Int. J. Multiphase Flow 20, 219–233.

Larson, T.K., Oh, C.H., Chapman, J.C., 1994. Flooding in a thin rectangular slit geometry representative of ATR fuel assembly side-plate flow channels. Nucl. Eng. Des. 152, 277–285.

McQuillan, K.W., Whalley, P.B., Hewitt, G.F., 1985. Flooding in vertical two-phase flow. Int. J. Multiphase Flow 11, 741–760.

No, H.C., Jeong, J.H., 1996. Flooding correlation based on the concept of hyperbolicity breaking in a vertical annular flow. Nucl. Eng. Des. 166, 249–258.

Nusselt, N., 1916. Die Oberflachenkondensation der Wasserdampfes. Zeit. Ver. D. Ing. 60, 541–569.

O'Brien, S.A., Such, D.K., Mills, A.F., 1986. The effect of liquid flow rate on flooding in vertical annular countercurrent two-phase 4 flow. Int. J. Multiphase Flow 12, 699–704.

Osakabe, M., Kawasaki, Y., 1989. Top flooding in thin rectangular and annular passages. Int. J. Multiphase Flow 15, 747–754.

Pushkina, O.L., Sorokin, Y.L., 1969. Breakdown of liquid film motion in vertical tubes. Heat Transfer Sov. Res. 1, 56–64.

Richter, H.J., 1981. Flooding in tubes and annuli. Int. J. Multiphase Flow 7, 647–658.

Shearer, C.J., Davidson, J.F., 1965. The investigation of a standing wave due to gas blowing upwards over a liquid film; its relation to flooding in wetted-wall columns. J. Fluid Mech. 22, 321–335.

Wallis, G.B., 1969. One-dimensional Two-phase Flow. McGraw-Hill, New York.

Wongwises, S., Thanaporn, R. 1998. Experimental and theoretical investigation of countercurrent flow limitation in inclined pipes. In: Presented at Third International Conference On Multi-phase Flow, ICMF'98, Lyon, France.

Zabaras, G.J. 1985. Studies of vertical annular gas–liquid flows. Ph.D. Thesis, University of Houston.

Zapke, A., Kroeger, D.G., 1996. The influence of fluid properties and inlet geometry on flooding in vertical and inclined tubes. Int. J. Multiphase Flow 22, 461–472.